VISUAL SERVOING FOR AN UNDERACTUATED MANIPULATOR

A. Espejel-Rivera * **L.E. Ramos-Velasco** *,1
S. Čelikovský **,2

* *Centro de Investigación en Tecnologías de Información y Sistemas. Universidad Autónoma del Estado de Hidalgo. Carr. Pachuca-Tulancingo, Km. 4.5 C.P. 42084, Pachuca, Hidalgo, México, aespejel@hotmail.com, lramos@uaeh.reduaeh.mx*
** *Institute of Information Theory and Automation, Academy of Sciences of the Czech Republic. P.O. Box 18, 182 08 Prague, Czech Republic, celikovs@utia.cas.cz*

Abstract: This paper discusses the visual servo control of an underactuated mechanism under fixed-camera configuration. The control goal is to stabilize the system over a desired static target by using a vision system equipped with a fixed camera to observe the system and target. We present a control scheme based on the combination of a state observer and the visual feedback for an underactuated system, the so-called *Pendubot*, consisting in a double pendulum actuated only at the first joint. The paper ends with the presentation of several simulation results and some guidelines for future work are drawn in the conclusion.

Keywords: Underactuated systems, visual servoing, nonlinear systems, Pendubot.

1. INTRODUCTION

In the past few years, there has been a considerable amount on interest in the control of underactuacted systems. Underactuated mechanical systems are systems with fewer independent control actuators than degrees of freedom to be controlled. The interest comes from the need to stabilize systems like ships, underwater vehicles, helicopters, aircraft, airships, hovercrafts, satellites, walking robots, etc, which may be underactuated by design. Actuators are expensive and/or heavy and are therefore avoided in a system design. Other systems may also become underactuacted due to actuator failure. Several control strategies based on passivity, Lyapunov theory, feedback linearization, output regulation, etc. have been developed for the fully actuated case, i.e. systems with the same number of actuators as degree of freedom (Craig, 1989; Isidori, 1995; Spong and Vidyasagar, 1989). The techniques developed for fully actuated robots do not apply directly to the case of underactuated mechanical systems (Chung and Hauser, 1995; Fantoni, et al., 2002; Lozano and Fatoni, 2002; Ramos, et al., 1998; Ramos, et al., 1997; Ramos, et al., 2002; Reyhanoglu, et al., 1999; Shim, et al., 1998; Spong, 1989; Spong, 1994; Spong, 1995). A visual solution to an actuator failures may be achieved by equipping the

---

[1] This work was supported in part by UAEH under research program UAEH-DIP-ICBI-AACC-103 and by PROMEP under research program 103.5/03/1130.
[2] Supported by the Grant Agency of the Czech Republic through the research grant No. 102/02/0709.

underactueted system with visual sensors. The use of a visual sensor in feedback control loops with robot manipulators represents an attractive solution to position and motion control (Andersen, et al., 1991; Andersson, 1990; Corke, 1996; Corke, et al. , 1996). Visual servoing is the use of vision as a high speed sensor, given many measurements or samples per second to close the robot's position loop. The camera may be stationary or held in the robot's "hand", the latter providing endpoint relative positioning information directly in the Cartesian or task space. Most existing generalizations of classical visual servoing techniques exploit a high gain or computed torque feedback to make a dynamic reduction of the system to a controllable kinematic model for which the visual servoing task may be solved directly (Corke, 1996). The dynamics model of a system is commonly ignored in the design of visual servo systems and closed-loop performance may be severely limited to ensure that the dynamic reduction is valid. Recently in (Kelly, 1996) has explored a more nonlinear aspect of the system dynamics, and presented an asymptotically stable method for position regulation for fixed-camera visual servoing. The difficulties associated with controlling an underactuated system have received even less attention. In (Zhang, 1999) has been working on the visual servoing problem using a Lagrangian representation of the system dynamics and consider underactuated and nonholonomic systems. In (Hamel and Mahony, 2000) proposed a new image-based control strategy for visual servoing which is applicable to a class of underactuated dynamic systems. While many interesting techniques and results have been presented for underactuacted systems, the control of these systems still remains an open problem. Important issues are: how can visual servoing be formulated for such systems; using the full nonlinear dynamics, how can closed-loop control problem be solved. These two issues are addressed in this paper. We

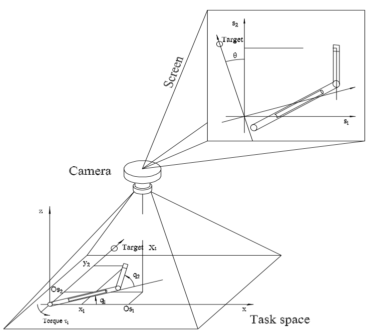

Fig. 1. Schematic representation of the Robot-camera system

develop a dynamic controller using visual sensor for an underactuated dynamic system which operate with accurate target information as shown in Figure 1. The proposed approach is motivated by a theoretical analysis of the dynamic equation of motion of a rigid body and exploits structural linear properties of these dynamics to derive a nonlinear observer and a linear control algorithm.

The paper is organized in the following manner. Section 2 describes the equivalent representation of the robot manipulator model while section 3 is devoted to the nonlinear observer structure. Section 4 gives the Pendubot model, where it is used in Section 5 to design a controller. In section 6 shows some simulation results. Finally, concluding remarks are given in Section 7.

2. EQUIVALENT REPRESENTATION OF THE ROBOT MODEL

The dynamic equation of an n degree-of-freedom robot manipulator in the continuos time can be written as (Spong, 1989)

$$\boldsymbol{D}(\boldsymbol{q})\,\ddot{\boldsymbol{q}} + \boldsymbol{C}(\boldsymbol{q}, \dot{\boldsymbol{q}}) + \boldsymbol{G}(\boldsymbol{q}) = \tau \qquad (1)$$

where $\boldsymbol{q}$ is the $(n\times 1)$ vector of joint variables (generalized coordinates), $\boldsymbol{D}(\boldsymbol{q})$ is the $(n\times n)$ symmetric positive-definite inertia matrix, $\boldsymbol{C}(\boldsymbol{q}, \dot{\boldsymbol{q}})$ is the vector of Coriolis and centripetal torques, $\boldsymbol{G}(\boldsymbol{q})$ are the gravitational terms, and τ is the $(n\times 1)$ vector of input torques.

Choosing as state vector $\boldsymbol{x} = \begin{pmatrix} \boldsymbol{x}_1^T & \boldsymbol{x}_2^T \end{pmatrix}^T = \begin{pmatrix} \boldsymbol{q}^T & \dot{\boldsymbol{q}}^T \end{pmatrix}^T$, as input $u = \tau$ and output y, the description of the system can be given in state space form as:

$$\dot{\boldsymbol{x}}_1 = \boldsymbol{x}_2 \qquad (2)$$

$$\dot{\boldsymbol{x}}_2 = -\boldsymbol{D}^{-1}(\boldsymbol{x}_1)[\boldsymbol{C}(\boldsymbol{x}_1, \boldsymbol{x}_2) + \boldsymbol{G}(\boldsymbol{x}_1)] + \boldsymbol{D}^{-1}(\boldsymbol{x}_1)u \qquad (3)$$

$$y = \boldsymbol{H}\boldsymbol{x} \qquad (4)$$

or

$$\dot{\boldsymbol{x}} = \boldsymbol{A}\boldsymbol{x} + \boldsymbol{B}(\boldsymbol{x})\,u + \boldsymbol{d}(\boldsymbol{x}) \qquad (5)$$

$$y = \boldsymbol{H}\boldsymbol{x} \qquad (6)$$

where

$$\boldsymbol{A} = \begin{bmatrix} \mathcal{O}_{n\times n} & \mathcal{I}_{n\times n} \\ \mathcal{O}_{n\times n} & \mathcal{O}_{n\times n} \end{bmatrix}, \quad \boldsymbol{B}(\boldsymbol{x}) = \begin{bmatrix} \mathcal{O}_{n\times n} \\ \boldsymbol{D}^{-1}(\boldsymbol{x}_1) \end{bmatrix},$$

$$\boldsymbol{d}(\boldsymbol{x}) = \begin{bmatrix} \mathcal{O}_{n\times n} \\ -\boldsymbol{D}^{-1}(\boldsymbol{x}_1)[\boldsymbol{C}(\boldsymbol{x}_1, \boldsymbol{x}_2) + \boldsymbol{G}(\boldsymbol{x}_1)] \end{bmatrix}.$$

where $\mathcal{O}_{n\times n}$ is the $(n\times n)$ null matrix, $\mathcal{I}_{n\times n}$ is the $(n\times n)$ identity matrix.

2.1 Discrete-time state-space equation

Visual servoing employs discrete-time model. Robot discrete-time dynamics has been studied by many researchers (Lai, et al., 1997; Mareels, et al., 1992; Neuman, et al., 1985; Nicosia, et al., 1986). To obtain a discrete-time state-space equation from a continuous-time state-space equation (5)-(6), we assume that all the measurements of the manipulator state are available at a sampling rate T, and the input torques are maintained constant between the sampling instants, i.e. over each time interval $\mathcal{I}_k = [kT \quad (k+1)T]$, where $k \geq 0$ is an integer, for sufficiently small time intervals $\dot{\boldsymbol{x}}$ can be approximated with a first forward difference, as follows:

$$\dot{\boldsymbol{x}} \approx \frac{\boldsymbol{x}(t+T) - \boldsymbol{x}(t)}{T} \tag{7}$$

Thus, the differential equation (5) can be expressed as (approximately)

$$\frac{\boldsymbol{x}(t+T) - \boldsymbol{x}(t)}{T} = \boldsymbol{A}\boldsymbol{x} + \boldsymbol{B}(\boldsymbol{x})\,u + \boldsymbol{d}(\boldsymbol{x}) \tag{8}$$

Solving this equation for $\boldsymbol{x}(t+T)$, we obtain

$$\boldsymbol{x}(t+T) = (\boldsymbol{I}+T\boldsymbol{A})\boldsymbol{x}(t) + T\boldsymbol{B}(\boldsymbol{x}(t))u(t) + T\boldsymbol{d}(\boldsymbol{x}(t)) \tag{9}$$

Evaluation of equations (9) and (6) at $t = kT$ yields a simple discrete-time model, based on the first order Euler method

$$\boldsymbol{x}[(k+1)T] = \Phi\boldsymbol{x}(kT) + \Gamma(\boldsymbol{x}(kT))u(kT) + \Psi(\boldsymbol{x}(kT)) \tag{10}$$

$$\boldsymbol{y}(kT) = \boldsymbol{H}\boldsymbol{x}(kT) \tag{11}$$

where

$$\Phi = (\boldsymbol{I} + T\boldsymbol{A}) \quad \Gamma = T\boldsymbol{B} \quad \Psi = T\boldsymbol{d}$$

3. STATE NONLINEAR OBSERVER DESIGN

We consider the problem of estimating the current state $\boldsymbol{x}(kT)$ of a nonlinear discrete-time dynamical system, described by a system of first-order-difference equations

$$\boldsymbol{x}[(k+1)T] = \Phi\boldsymbol{x}(kT) + \Gamma(\boldsymbol{x}(kT))u(kT) + \Psi(\boldsymbol{x}(kT)) \tag{12}$$

$$\boldsymbol{y}(kT) = \boldsymbol{H}\boldsymbol{x}(kT) \tag{13}$$

from the past observations $\boldsymbol{y}(sT)$, $s \leq k$, where the discrete-time index $k \in \{0, 1, 2, \ldots\}$ and T is the sampling period.

For the discrete-time manipulator model form (12)-(13), the proposed observer is given by

$$\widehat{\boldsymbol{x}}[(k+1)T] = \Phi\widehat{\boldsymbol{x}}(kT) + \Gamma(\boldsymbol{y}(kT))u(kT) + \Psi(\boldsymbol{y}(kT)) + \boldsymbol{K}_e[\boldsymbol{y} - \widehat{\boldsymbol{y}}(kT)] \tag{14}$$

$$\widehat{\boldsymbol{y}}(kT) = \widehat{\boldsymbol{x}}(kT) \tag{15}$$

The resulting error equation takes on the following form

$$\boldsymbol{e}(k+1) = (\Phi - \boldsymbol{K}_e\boldsymbol{H})\boldsymbol{e}, \qquad \boldsymbol{e} := \boldsymbol{x} - \widehat{\boldsymbol{x}} \tag{16}$$

As the pair $(\boldsymbol{H}, \Phi)$ is observable, the eigenvalues of the error system may be arbitrary assigned.

4. THE PENDUBOT AND CAMERA MODELS

The Pendubot, which is the underactuated system considered here, it is shown schematically in Figure 2. For the purposes of this work, we assume that it has a planar motion without friction.

Table 1. Parameters of the Pendubot.

notation		value	unit
Mass of link 1	m_1	0.5289	kg
Mass of link 2	m_2	0.3346	kg
Length of link 1	l_1	0.26987	m
Length of link 2	l_2	0.38417	m
Distance to the center of mass of link 1	l_{c_1}	0.13494	m
Distance to the center of mass of link 2	l_{c_2}	0.19208	m
Moment of inertia of link 1 about its centroid	I_1	0.013863	Kgm^2
Moment of inertia of link 2 about its centroid	I_2	0.016749	Kgm^2
Acceleration due to gravity	g	9.81	m/sec^2
Angle that link 1 makes with the horizontal	q_1		rad
Angle that link 2 makes with the link 1	q_2		rad
Torque applied on link 1	τ_1		$Nw-m$

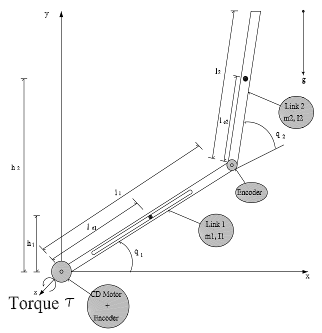

Fig. 2. The Pendubot system.

For the Pendubot system, the dynamic model (1) is particularized as

$$\begin{bmatrix} D_{11} & D_{12} \\ D_{12} & D_{22} \end{bmatrix} \begin{bmatrix} \ddot{q}_1 \\ \ddot{q}_2 \end{bmatrix} + \begin{bmatrix} C_1 \\ C_2 \end{bmatrix} + \begin{bmatrix} G_1 \\ G_2 \end{bmatrix} = \begin{bmatrix} \tau_1 \\ 0 \end{bmatrix} \tag{17}$$

where

$$
\begin{aligned}
D_{11} &= m_1 l_{c1}^2 + m_2 \left(l_1^2 + l_{c2}^2 + 2 l_1 l_{c2} \cos\left(q_2\right) \right) \\
&\quad + I_1 + I_2 \\
D_{12} &= m_2 \left(l_{c2}^2 + l_1 l_{c2} \cos\left(q_2\right) \right) + I_2 \\
D_{22} &= m_2 l_{c2}^2 + I_2 \\
C_1 &= -2 m_2 l_1 l_{c2} \dot{q}_1 \dot{q}_2 \sin\left(q_2\right) - m_2 l_1 l_{c2} \dot{q}_2^2 \sin\left(q_2\right) \\
C_2 &= m_2 l_1 l_{c2} \dot{q}_1^2 \sin\left(q_2\right) \\
G_1 &= m_1 g l_{c1} \cos\left(q_1\right) + m_2 g l_1 \cos\left(q_1\right) \\
&\quad + m_2 g l_{c2} \cos\left(q_1 + q_2\right) \\
G_2 &= m_2 g l_{c2} \cos\left(q_1 + q_2\right).
\end{aligned}
$$

4.1 Equivalent representation

Choosing as state vector $\boldsymbol{x} = \left(\boldsymbol{x}_1^T \ \boldsymbol{x}_2^T \right)^T = \left(x_1 \ x_2 \ x_3 \ x_4 \right)^T := \left(q_1 \ q_2 \ \dot{q}_1 \ \dot{q}_2 \right)^T = \left(\boldsymbol{q}_1^T \ \boldsymbol{q}_2^T \right)^T$, as input $u = (\tau_1 \quad 0)^T$ and q_2 as the output, the description of the system can be given in state space form (5)-(6), where:

$$
\boldsymbol{A} = \begin{bmatrix} 0 & 0 & 1 & 0 \\ 0 & 0 & 0 & 1 \\ 0 & 0 & 0 & 0 \\ 0 & 0 & 0 & 0 \end{bmatrix}, \quad \boldsymbol{B}(\boldsymbol{x}) = \frac{1}{\Delta} \begin{bmatrix} 0 & 0 \\ 0 & 0 \\ D_{22} & -D_{12} \\ -D_{12} & D_{11} \end{bmatrix},
$$

$$
\boldsymbol{d}(\boldsymbol{x}) = \frac{1}{\Delta} \begin{bmatrix} 0 \\ 0 \\ D_{12}(C_2 + G_2) - D_{12}(C_1 + G_1) \\ D_{12}(C_1 + G_1) - D_{11}(C_2 + G_2) \end{bmatrix},
$$

$$
\boldsymbol{H} = \begin{bmatrix} 1 & 1 & 0 & 0 \end{bmatrix}, \quad \Delta = D_{11} D_{22} - D_{12}^2.
$$

4.2 Discrete-time state-space

For the Pendubot model, the matrices Φ, Γ, Ψ for discrete-time state-space representation (10)-(11) are

$$
\Phi = \begin{bmatrix} 1 & 0 & T & 0 \\ 0 & 1 & 0 & T \\ 0 & 0 & 1 & 0 \\ 0 & 0 & 0 & 1 \end{bmatrix}, \quad \Gamma = T\boldsymbol{B} = \frac{T}{\Delta} \begin{bmatrix} 0 & 0 \\ 0 & 0 \\ D_{22} & -D_{12} \\ -D_{12} & D_{11} \end{bmatrix},
$$

$$
\Psi = T\boldsymbol{d} = \frac{T}{\Delta} \begin{bmatrix} 0 \\ 0 \\ D_{12}(C_2 + G_2) - D_{12}(C_1 + G_1) \\ D_{12}(C_1 + G_1) - D_{11}(C_2 + G_2) \end{bmatrix},
$$

$$
\boldsymbol{H} = \begin{bmatrix} 1 & 1 & 0 & 0 \end{bmatrix}.
$$

Here, $\boldsymbol{x}(kT)$ is the state vector (4-vector) at kth sampling instant, $u(kT)$ control signal (scalar) at kth sampling and $y(kT) = \boldsymbol{H}\boldsymbol{x}(kT)$ is the output at kth sampling. This provides an discrete-time state-space model that can be used in the design of state observers, as discussed in the section that follows.

4.3 Camera model

A detailed model of the visual system was established in (Corke, et al. , 1992). The transfer function of the visual system may be approximated by

$$
\frac{K_{lens}}{z^2(z-1)} \tag{18}
$$

where the pole at $z = 1$ is due to the software velocity control, and the two poles at the origin represent a delay due to pixel transport, communications and servo response. Finally, the lens introduce a target distance dependent gain, K_{lens}, due to perspective.

5. CONTROL SCHEME

Our goal is to use an external camera as sensor and use an nonlinear observer to estimate the state of the system and stabilize the Pendubot. In this section it is shown how a visual servoing control may be derived based on estimation techniques for a fix camera with underactuated rigid body dynamics. Visual servoing systems incorporate the visual sensors in the feedback. Figure 3 depicts a block diagram of the closed-loop control system, this is a block diagram of one degree of freedom (1-DOF). The camera lens is modelled as a simple gain, K_{lens}, which, due to perspective, is a function of target distance. We shall first discuss the full-order state observer and then the state feedback controller.

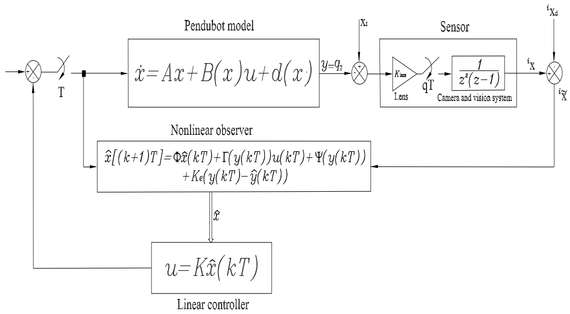

Fig. 3. Structure of visual servo control for the Pendubot. Here, X_t is the world coordinate location of the target, ^iX_d is the desired location of the target on the image plane, and $^i\tilde{X} = {}^iX - {}^iX_d$ is the image plane error.

5.1 State observer design

It is important to note that, in the present analysis, state $\boldsymbol{x}(kT)$ is not available by direct measurement. Since the output $\boldsymbol{y}(kT) = \boldsymbol{H}\boldsymbol{x}(kT)$ can be measured by the fix camera, we can design a state nonlinear observer (14)-(15) for the Pendubot model.

5.2 Controller design

When the Pendubot is in a neighborhood of its top unstable equilibrium position, a linear controller can stabilize the pendulum quite adequately. We know that the linearized system is observable and controllable, then it is possible to design a linear control (Ramos, 1997). Therefore, the control objective is to stabilize the system around its unstable equilibrium point $x^* = (x_1^*, x_2^*, x_3^*, x_4^*)^T = (\frac{\pi}{2}, 0, 0, 0)^T$, i.e. to bring the second pendulum to its upper position and the first angle q_1 to zero simultaneously. The observed state $\hat{x}(k)$ is used to form the vector control $u(k)$, or

$$u(k) = -K\hat{x}(k) \tag{19}$$

where K is the state feedback gain matrix.

6. SIMULATION RESULTS

In all the simulations, we consider that the initial condition of the system is near to the equilibrium point x^* and the gain K that stabilizes the linear approximation of the Pendubot model was obtained by solving a LQR problem

$$K = \begin{bmatrix} -22.4431 - 21.2982 - 6.2282 - 4.4932 \end{bmatrix}, \tag{20}$$

the observer feedback gain matrix

$$K_e = \begin{bmatrix} -2.9468 \\ 0.3185 \\ -18.6506 \\ 7.7243 \end{bmatrix} \tag{21}$$

and the lens gain

$$K_{lens} = 0.50. \tag{22}$$

We have used *Simulink*^{TM} and *MATLAB*^{TM} to simulate the full dynamic motion of the Pendubot. Figure 4 shows the trajectory of the target in the image plane with ${}^iX_d = 0$, for convenience.

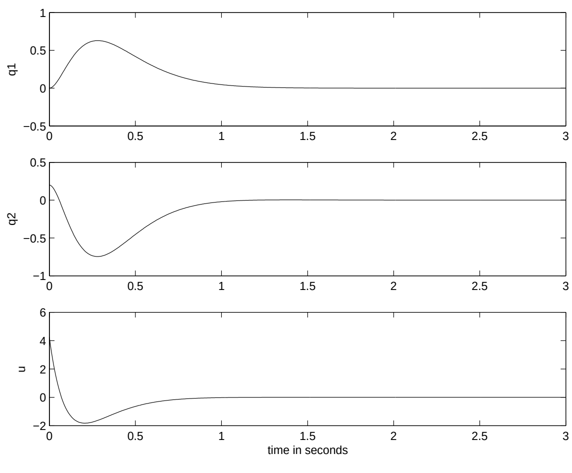

Fig. 4. Simulation results. Positioning with respect to the target $X_t = (0, 90°)$.

7. CONCLUSIONS AND FUTURE WORK

This paper presents an alternative approach to the design of discrete-time feedback controllers and state observer for an underactuacted manipulators using a visual feedback. The case studied is the so-called *Pendubot*, consisting in a double pendulum actuated only at the first joint. The control of the Pendubot is specially difficult since it is an underactuated mechanism (two degrees of freedom and only one input). In this work, we have presented a linear position tracking controller for a fixed camera vision-based, Pendubot system. Specifically, by assuming exact knowledge of the mechanical parameters, and by considering an accepted camera model together with the robot non linear dynamics, we have proposed an image-based visual servoing scheme derived from based on the combination of an non linear observer and the visual feedback, the design shows that this controller provides a good performance when balancing the links about the unstable vertical position. Numerical simulations assuming a discrete-time implementation of the visual controller showed the performance of the closed loop system. Preliminary results indicate that visual servoing is potentially attractive alternative for underactuated systems. We are currently implementing the algorithm on a Texas Instruments TMS320C6711 digital signal processor based system.

REFERENCES

Andersen, N.A., O. Ravn and A.T. Sorensen (1991). Real-time vision based control of servomechanical systems. In: *2nd International Symposium Experimental Robotics.*

Andersson, R.L. (1990). Alow-latency 60 hz stero vision system for real-time visual control. In: *5th International Symposium on Intelligent Control.*

Chung, C.C. and J. Hauser (1995). Nonlinear control of a swinging pendulum, *Automatica*, **31**, 851-862.

Corke, P.I. and M.C. Good (1992). Dynamic effects in high-performance visual servoing. In: *Proceedings of the IEEE Int. Conf. Robotics and Automation*, Nice, France, 1838-1843.

Corke, P.I., G.D. Hager and S. Hutchinson (1996). *Visual control of robots: high-performance servoing.* John Wiley, Great Britain.

Corke, P.I., G.D Hager and S. Hutchinson (1996). A Tutorial on Visual Servo Control, *IEEE Transactions on Robotics and Automation*, **12**, 651-670.

Craig, J.J. (1989). *Introduction to Robotics: mechanics and control.* Addison-Wesley.

Fantoni, I. and R. Lozano (2002). *Non-linear Control for Underactuated Mechanical System.* Springer Verlang, London.

Hamel, T. and R. Mahony (2000). Visual servoing of a class of under-actuated dynamic rigid-body system. In: *Proceedings of the 39th IEEE Conference on Decision and Control*, Sydney, Australia.

Isidori, A. (1995). *Nonlinear Control Systems.* Springer-Verlag, New York.

Kelly, R. (1996). Robust Asymptotically Stable Visual Servoing of Planar Robots, *IEEE Transactions on Robotics and Automation*, **12**, 759-766.

Lai, R., Y. Yamanaka, F. Ohkawa and R. Katoh (1997). Digital control of a robot manipulator disturbed by unknown external forces. In: *Proceeding of the Society if Instruments and control Engineers, SICE'97*, Tokushima, Japan, 1115-1118.

Lozano, R. and I. Fantoni (2002). Stabilization of the inverted pendulum around its homoclinic orbit, *System and Control Letters*, **40**, 197-204.

Mareels, I., H.B. Penfold and R.J. Evans (1992). Controlling nonlinear time-varying systems via Euler approximations, *Automatica*, **28**, 681-696.

Neuman, C.P., and V.D. Tourassis (1985). Discrete dynamic robot models, *IEEE Transactions on Systems, Man and cybernetics, SMC*, **15**, 193-204.

Nicosia, S., P. Tomei and A. Tornambe (1986). Discrete dynamics of robot arm. In: *Poceedings of IFAC Theory of Robotics.*

Ramos, L.E., B. Castillo-Toledo and S. Negrete (1998). Nonlinear regulation of a seesaw-inverted pendulum. In: *Proceedings of the IEEE ICCA*, Trieste, Italy.

Ramos, L.E., B. Castillo-Toledo and J. Álvarez (1997). Nonlinear regulation of an underactueted system. In: *Proceedings of the IEEE ICRA*, Albuquerque, New Mexico, 3288-3293.

Ramos-Velasco, L.E., J.J Ruíz-León and S. Celikovský (2002). Rotary Invertd Pendulum: Trayectory tracking via nonlinear control techniques, *Kybernetika*, **38**, 217-232.

Reyhanoglu, M., A.J. van der Schaft, N.H. McClamroch and I. Kolmanovsky (1999). Dynamics and control of a class of underactuated mechanical systems, *IEEE Transactions on Automatic Control*, 1663-1671.

Shim, H., T. Koo, F. Hoffmann and S. Sastry (1998). A comprehensive study of control design for an autonomous helicopter. In: *Proceedings of the 37th IEEE Conference on Decision and control CDC'98.*

Spong, M.W. and M. Vidyasagar (1989). *Robot Dynamics and Control.* John Wiley and Sons, New York.

Spong, M.W. (1994). The swing up control of the acrobot. In: *IEEE International Conference on Robotics and Automation*, San Diego, CA.

Spong, M.W. and D.J. Block (1995). The pendubot: A mechatronic system for control research and education. In: *Poceedings of the 34th IEEE Conference on Decision and Control.*

Zhang, H. and J.P Ostrowski (1999). Visual Servoing with Dynamics: Control of an Unmanned Blimp. In: *IEEE International Conference on Robotics and Automation*, Detroit, Michgan.